

## ON THE OPTIMIZATION OF PRECIPITATED AUSTENITE FOR TRANSFORMATION TOUGHENING OF STEELS

G.N. Haidemenopoulos<sup>1</sup>, M. Grujicic<sup>2</sup>, G.B. Olson<sup>3</sup>, and Morris Cohen<sup>4</sup>

1. Metallurgical Industrial Research and Technology Center (MIRTEC), 38500 Volos, Greece
2. Department of Mechanical Engineering, Clemson University, Clemson, SC
3. Department of Materials Science and Engineering, Northwestern University, Evanston, IL
4. Department of Materials Science and Engineering, Massachusetts Institute of Technology, Cambridge MA

**ABSTRACT** The most important factors affecting the dispersed-phase transformation toughening in steels are the stability of the dispersed austenite and the transformation volume change. Both depend on the composition of the steel. The THERMOCALC computer program was used to describe the effect of composition on austenite stability while a formulation based on the two-gamma states model allowed the description of the compositional dependence of the lattice parameters taking into account magneto-volume effects in the austenite.

### 1. Introduction

The interaction of deformation-induced martensitic transformation with fracture-controlling processes, such as microvoid-induced shear localization, results in a toughening mechanism termed dispersed-phase transformation toughening. The transformation behavior and the toughening effects are controlled by the stability of the austenitic dispersion, the most microstructural parameters being the size and the chemical composition of the austenite particles. These effects have been studied recently in high Ni-Co secondary hardening martensitic steels and in particular AF1410 steel [1,2]. Enhanced transformation toughening at ultrahigh-strength levels (>2 GPa), requires a large transformation volume change. Recent experiments by Young [3] on phosphocarbide-strengthened austenitic steels demonstrated a significant contribution of the transformation volume change  $\Delta V/V$  to the toughness increment due to transformation toughening.

In quantitative terms, for transformation toughening to occur, the austenite dispersion must have the optimum degree of stability for the crack-tip stress state. The optimum stability is quite high due to the high triaxiality ahead of the crack tip. This condition then prescribes the microstructural requirements, i.e., austenite particle size and composition, to obtain this degree of stability. Thermodynamic calculations can then be used to select alloy compositions that achieve this stability of the precipitated austenite.

The alloy design procedure, outlined above, is then subjected to the constraint that the alloy compositions selected should maximize the transformation volume change. Alloy compositions affect the volume change through the composition dependence of the lattice parameters of the austenite and martensite. Magnetic changes, such as ferromagnetism and the INVAR effect, become important in the austenite, which can reduce the transformation volume change and the resulting toughening.

It is, therefore, important to select alloy compositions that ensure high austenite stability while promoting a large transformation volume change. This then establishes the framework for alloy design to achieve transformation toughening.

### 2. Austenite Stabilization

Since the steel is designed for transformation toughening at room temperature, a quantitative characterization of austenite stability that can also be used for alloy design can be provided by the free-energy

change for martensitic transformation evaluated at room temperature. This quantity  $\Delta G^{\text{ch}}(\text{RT})$  was calculated for the Fe-Ni-Co system. The martensitic phase was represented by the BCC phase with the same composition as FCC since the transformation is diffusionless. Fig.1 shows the contours of the free energies of FCC and BCC as a function of composition, evaluated at 300K. The difference between these free energies is the free-energy change for the martensitic transformation  $\Delta G^{\text{ch}} = G^{\text{bcc}} - G^{\text{fcc}}$ . The more positive this quantity, the more stable the austenite. Fig.2 shows contours of  $\Delta G^{\text{ch}}$  as a function of composition for the ternary Fe-Ni-Co system. Superimposed on the same plot is the isothermal section of Fe-Ni-Co at 510°C (dotted lines) with two tie-lines shown. This combined plot allows one to select alloy compositions for austenite stabilization. Starting with an alloy composition  $X_0$ , the corresponding tie-line defines the composition of the austenite  $X_\gamma$  that precipitates at 510°C. That composition then defines, from the  $\Delta G^{\text{ch}}$  contour plot, the chemical driving force at room temperature. Therefore, alloy compositions that maximize austenite stability can be selected.

### 3. Transformational Volume Change

#### 3.1 General Considerations

The transformational volume change is subjected to some control through the composition dependence of the lattice parameters of austenite and martensite. Alloy compositions can then be designed that result in high  $\Delta V/V$  and, hence, enhanced toughening. The volume change resulting from the martensitic transformation FCC  $\rightarrow$  BCC is related to the lattice parameters  $\alpha_{\text{FCC}}$  and  $\alpha_{\text{BCC}}$  of the two phases as:

$$\frac{\Delta V}{V} = 2 \left[ \frac{\alpha_{\text{BCC}}}{\alpha_{\text{FCC}}} \right]^3 - 1 \quad (1)$$

The lattice parameters are functions of composition:

$\alpha_{\text{FCC}} = f_1(X_i)$ ,  $\alpha_{\text{BCC}} = f_2(X_i)$ ,  $i = \text{Fe, Co, Ni, Cr}$  ( the carbon content of the precipitated austenite in AF1410 steel is negligibly small )

where  $X_i$  is the mole fraction of element  $i$ . In particular, the form of the function  $f_1$  for the FCC phase is influenced by magnetic changes, such as volume magnetostriction and the INVAR effect, both of which increase the value of  $\alpha_{\text{FCC}}$  and, hence, reduce  $\Delta V/V$ . An attempt will be made here to develop analytical expressions for  $\alpha_{\text{FCC}}$  taking into account these magnetic effects. The two-gamma states formalism developed by Tauer and Weiss[4] is used to describe the INVAR effect on  $\alpha_{\text{FCC}}$

#### 3.2 The Two-Gamma States Model.

In a study designed to separate the contribution of magnetic structure to phase transformations, Tauer and Weiss[5,6] attempted an analysis of the specific heat of various substances, including iron, by separation into magnetic, electronic, and lattice contributions. In order to equate the free energy of BCC and FCC iron at the  $\alpha/\gamma$  transition at 910°C, it was necessary to postulate a sizeable magnetic entropy term for  $\gamma$ -iron, which was inconsistent with the absence of a specific heat anomaly at the Néel temperature. The high-temperature properties of  $\gamma$ -iron suggested ferromagnetic behavior with a large saturation magnetic moment, while the low-temperature properties suggested antiferromagnetic behavior with a much smaller magnetic moment. It was therefore proposed that there existed two discrete electronic states of  $\gamma$ -iron,  $\gamma_1$  and  $\gamma_2$ , separated by a specific energy difference in equilibrium with each other in a manner corresponding to a two-level Schottky excitation[7]. Individual atoms are not considered to permanently possess either of the electronic configurations, but have a probability of exhibiting both states on a time-transient basis according to the ratio:

$$a = \frac{f}{1-f} = (g_1/g_0) \exp\left(-\frac{\Delta E}{RT}\right) \quad (2)$$

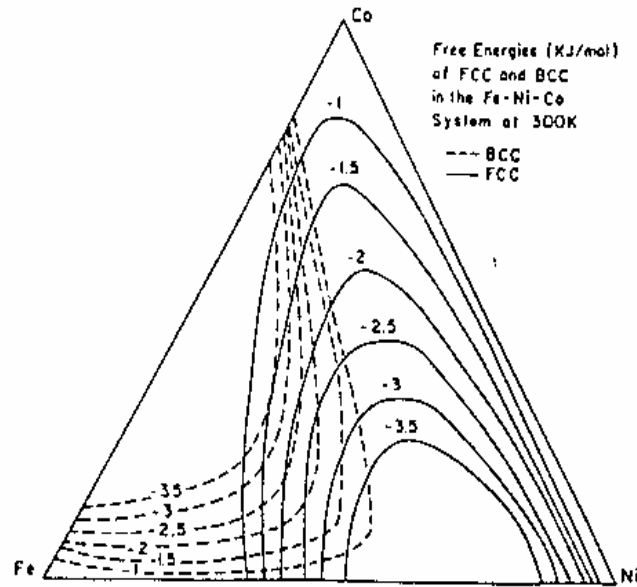


FIG. 1

Free Energy Contours (in KJ/Mol) of the FCC and BCC phases in the Fe-Ni-Co system at 300K.

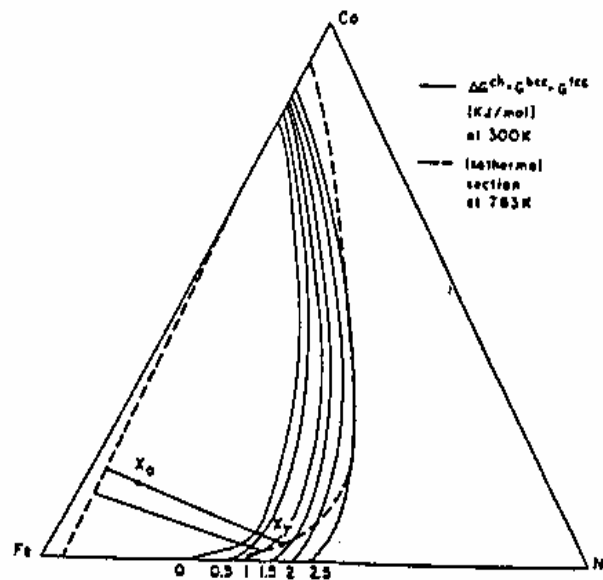


FIG. 2

Contours of the free energy change (in KJ/Mol) for the martensitic transformation at 300K (solid lines) and superimposed isothermal section (dotted lines) at 783K of the Fe-Ni-Co system.  $X_0$  represents the alloy composition and  $X_y$  the austenite composition.

where  $a$  is the probability of the upper energy state being occupied and  $f$  the corresponding fraction of iron atoms in the upper energy state.  $\Delta E$  represents the energy difference between the two states and  $g_0$  and  $g_1$  the degeneracies of the upper and lower states respectively. The properties of the  $\gamma_1$  and  $\gamma_2$  states are presented in Table 1. In pure  $\gamma$ -iron, the antiferromagnetic (low volume) state is the ground state ( $T=0K$ ). Addition of Ni, Co, and Cr reverses the relative stability between  $\gamma_1$  and  $\gamma_2$  promoting the ferromagnetic (high volume)  $\gamma_2$  state. On the other hand, addition of Mn stabilizes the  $\gamma_1$  state [6,8].

**Table 1** Approximate values of lattice parameter, spin per atom, and Curie or Néel temperature of the two electronic structures of gamma-iron (reference 8).

	Crystal Structure	Lattice Parameter	Magnetic Structure	Spin per Atom ( $\mu_B$ )	Curie or Néel Temp.
$\gamma_1$	FCC	3.54 Å	Anti-Ferro	0.5	80 K
$\gamma_2$	FCC	3.64	Ferro	2.8	1800 K

### 3.3 Lattice Parameters.

The formulation of the compositional dependence of the lattice parameter  $\alpha_{FCC}$  is based on the description of two composition-dependent effects:

1. the effect of composition on the relative occupancy of the  $\gamma_1$  and  $\gamma_2$  states through the compositional dependence of  $\Delta E$ , the energy difference between the two gamma states and;
2. the effect of composition on the overall magnetic moment, which influences the magnitude of volume magnetostriction.

These effects are studied in the Fe-Ni-Co-Cr system with the following procedure: an expression for the lattice parameter is derived in the Fe-Ni binary system which is adopted as a reference. Then the effect of Cr and Co on both the relative stability of  $\gamma_1$  and  $\gamma_2$  states and the magnetic moment is considered, to derive the final expression for  $\alpha_{FCC}$ .

Using Vegard's law, the lattice parameter  $\alpha$  for the Fe-Ni system is:

$$\alpha_{FCC} = (1 - X_{Ni}) \left[ \alpha_{\gamma_2} \cdot f_{\gamma_2} + \alpha_{\gamma_1} \cdot f_{\gamma_1} \right] + X_{Ni} \alpha_{Ni} \quad (3)$$

where  $f_{\gamma_1}$  and  $f_{\gamma_2}$  are the fractions of iron atoms in the  $\gamma_1$  and  $\gamma_2$  states respectively as defined by eq(2), and  $\alpha_{\gamma_1}, \alpha_{\gamma_2}$  are the lattice parameters of the  $\gamma_1$  and  $\gamma_2$  states given in Table 1.  $X_{Ni}$  and  $\alpha_{Ni}$  are the mole fraction and lattice parameter of Ni respectively. According to data on the composition dependence of  $\Delta E$  by Weiss[6],  $\Delta E=0$  at  $X_{Ni}=0.29$ . Therefore, for  $X_{Ni}>0.29$  the  $\gamma_2$  state is stable. In order to develop eq(3) further, an analytical expression for  $\Delta E(X_{Ni})$  is required. The following expression was assumed:

$$\Delta E = A + B X_{Ni} + C X_{Ni}^2 + D X_{Ni}^3 + E X_{Ni}^4 \quad (4)$$

This expression was fitted to data on  $\Delta E$  vs  $X_{Ni}$  reported by Weiss[6], giving  $A=-820$ ,  $B=658.85$ ,  $C=-11107.9$ , and  $D=62030$  for  $X_{Ni}<0.29$ , and  $A=-1.07 \times 10^6$ ,  $B=1.28 \times 10^6$ ,  $C=-5.71 \times 10^6$ ,  $D=1.11 \times 10^7$ , and  $E=-8.03 \times 10^6$  for

$0.29 < X_{Ni} < 0.45$ . Having established the compositional dependence of  $\Delta E$ , the lattice parameter  $\alpha_{FCC}$  in the Fe-Ni system is found to be:

$$\alpha_{FCC} = 3.54 \left[ 1 - \lambda_1 X_{Ni} + \frac{\lambda_2 (1 - X_{Ni})}{1 + g/1.79} \right] \text{ for } X_{Ni} < 0.29 \quad (5a)$$

$$\alpha_{FCC} = 3.64 \left[ 1 - \lambda_1' X_{Ni} - \frac{\lambda_2' (1 - X_{Ni})}{1 + g} \right] \text{ for } X_{Ni} > 0.29 \quad (5b)$$

with  $g = \exp(\Delta E/RT)$  and  $\lambda_1 = 0.0075$ ,  $\lambda_2 = 0.0293$ ,  $\lambda_1' = 0.0338$ , and  $\lambda_2' = 0.0273$ .  $\Delta E$  is given by eq(4). Fig.3 presents the lattice parameter  $\alpha_{FCC}$  as a function of mole fraction Ni in the Fe-Ni system for  $X_{Ni} < 0.29$  (Fig.3a) and  $0.29 < X_{Ni} < 0.5$  (Fig.3b). Stabilization of the high-volume ferromagnetic  $\gamma_2$  state with the addition of Ni, as depicted in Fig.3b, results in an increase in the lattice parameter in the composition range  $X_{Ni} = 0.30$  to 0.40. However, with further addition of Ni, the  $\gamma_2$  state becomes saturated and the effect of the low-volume Ni becomes evident in reducing the lattice parameter above  $X_{Ni} = 0.40$ . The data presented here for the lattice parameter of the Fe-Ni system are in very good agreement with experimental data obtained by Ruhl[9].

#### Effect of Chromium

Addition of Cr markedly reduces the saturation magnetization[10], which results in a decrease in the lattice parameter irrespective of Ni content. However, Cr stabilizes the  $\gamma_2$  high-volume state and, therefore, the transition from  $\gamma_1$  to  $\gamma_2$  occurs at lower Ni contents ( $X_{Ni} < 0.29$ ). The data of Miodownik[10] for  $\Delta E$  vs  $X_{Cr}$  in the Fe-Ni-Cr system were fitted to an expression of the form:

$$\Delta E = A' + B' X_{Cr} + C' X_{Cr}^2$$

yielding  $A' = 50$ ,  $B' = 9180$ , and  $C' = -50800$ , while  $\Delta E$  is in cal/mol. Then, with Vegard's law, the lattice parameter  $\alpha_{FCC}$  in the Fe-Ni-Cr system becomes:

$$\alpha_{FCC} = 3.64 \left[ 1 - \lambda_1' X_{Ni} - X_{Cr} + \frac{\lambda_2' (1 - X_{Ni} - X_{Cr})}{1 + \frac{g_1}{g_0} \exp(-\Delta E/RT)} \right] \quad (6.6)$$

$$+ X_{Cr} \left[ C_1 - C_2 (X_{Ni} - C_3)^2 + C_4 (X_{Ni} - C_3)^4 \right]$$

Eq(6) was fitted to experimental data of Pearson[11] for lattice parameters in the Fe-Ni-Cr system to give  $C_1 = 3.433$ ,  $C_2 = 2.838$ ,  $C_3 = 0.506$ , and  $C_4 = -162.605$ .

#### Effect of Cobalt

The effect of Co on the lattice parameter  $\alpha_{FCC}$  will now be examined. Co stabilizes the  $\gamma_2$  high-volume state. It also increases the saturation magnetic moment, which should lead to larger lattice parameters. From ref.6,  $\Delta E = 0$  at  $X_{Co} = 0.4$  in the Fe-Co system. The  $\Delta E$  vs  $X_{Co}$  curve can be derived from the  $\Delta E$  vs  $X_{Ni}$  curve by substituting  $X_{Ni} = X_{Co}(0.29/0.40)$  in eq(4). The result is:

$$\Delta E = A'' + B'' X_{Co} + C'' X_{Co}^2 + D'' X_{Co}^3 \quad (7)$$

where  $A'' = -820$ ,  $B'' = 594.5$ ,  $C'' = -8053.2$ , and  $D'' = 44971.7$ . Eq(7) then represents the effect of Co on the relative stability between the  $\gamma_1$  and  $\gamma_2$  states. The magnetic moment (in Bohr magnetons) was calculated for the FCC phase in the Fe-Ni-Co-Cr system using the following equation:

$$B = \sum_i X_i B(\text{FCC}, i, 0) + \sum_{i,j} X_i X_j \left[ B(\text{FCC}, i, j, 0) + (X_i - X_j) B(\text{FCC}, i, j, 1) + (X_i - X_j)^2 B(\text{FCC}, i, j, 2) + \dots \right]$$

where  $i, j = \text{Co, Cr, Fe, Ni}$ , and  $B(\text{FCC}, i, j)$  are defined in the THERMOCALC database[12] and their values are given in Table 2.

**Table 2** Coefficients  $B(\text{FCC}, i, j)$  in Bohr magnetons for the magnetic moments defined in the THERMOCALC database.

Magnetic Moment	Value
$B(\text{FCC}, \text{Fe}; 0)$	-2.1
$B(\text{FCC}, \text{Ni}; 0)$	0.52
$B(\text{FCC}, \text{Co}; 0)$	1.35
$B(\text{FCC}, \text{Cr}; 0)$	-2.1
$B(\text{FCC}, \text{Fe}, \text{Ni}; 0)$	9.55
$B(\text{FCC}, \text{Fe}, \text{Ni}; 1)$	7.23
$B(\text{FCC}, \text{Fe}, \text{Ni}; 2)$	5.93
$B(\text{FCC}, \text{Fe}, \text{Ni}; 3)$	6.18
$B(\text{FCC}, \text{Co}, \text{Fe}; 0)$	9.74
$B(\text{FCC}, \text{Co}, \text{Fe}; 1)$	-3.51
$B(\text{FCC}, \text{Co}, \text{Ni}; 0)$	1.04
$B(\text{FCC}, \text{Co}, \text{Ni}; 1)$	0.16
$B(\text{FCC}, \text{Cr}, \text{Ni}; 0)$	-1.91

Fig.4 shows the variation of the magnetic moment with Ni content for the Fe-Ni, Fe-Ni-5Co, and Fe-Ni-5Cr systems evaluated using eq(8). The contribution of the magnetic moment to the lattice parameter of Fe-Ni-Cr can now be calculated with the aid of eq(6). For  $X_{\text{Ni}} = 0.4$  and  $X_{\text{Cr}} = 0.05$  this equation gives  $\alpha_{\text{FCC}} = 3.5775 \text{ \AA}$ , while excluding the last term in brackets (eq.6) from the calculation (representing the effect of the magnetic moment) gives  $\alpha_{\text{FCC}} = 3.5924 \text{ \AA}$ . Therefore, the addition of 5% Cr reduces the lattice parameter by  $\Delta\alpha = 0.01495 \text{ \AA}$ . This reduction in the lattice parameter is due to a reduction in the magnetic moment  $\Delta B$  caused by the addition of 5% Cr. The value of  $\Delta B$  is 0.35 from Fig.3 for  $X_{\text{Ni}} = 0.40$ . Therefore,  $\Delta\alpha = (0.01495/0.35) \Delta B$  or  $\Delta\alpha = 0.04271 \Delta B$ , where  $\Delta\alpha$  is in  $\text{ \AA}$  and  $\Delta B$  is in Bohr magnetons. To find the corresponding effect of Co, the value of  $\Delta B$  at  $X_{\text{Ni}} = 0.40$  was evaluated from the curves for Fe-Ni and Fe-Ni-5Co of Fig.3. This gave  $\Delta B = 0.1$ . Assuming the relation between  $\Delta\alpha$  and  $\Delta B$  above to hold for Co as well, we obtain  $\Delta\alpha = 0.04271 \times (0.1/0.05) X_{\text{Co}}$  or  $\Delta\alpha = 0.08542 X_{\text{Co}}$ . This equation represents the effect of the magnetic moment on the lattice parameter due to addition of Co.

Taking all the above into consideration, the lattice parameter  $\alpha_{\text{FCC}}$  for the Fe-Ni-Cr-Co system is given by Vegard's law (and using eq(6)) as:

$$\alpha_{\text{FCC}} = 3.514 X_{\text{Ni}} + 3.544 X_{\text{Co}} + X_{\text{Fe}} \left[ f_{\gamma_1} \alpha_{\gamma_1} + f_{\gamma_2} \alpha_{\gamma_2} \right] \quad (8)$$

$$+ X_{\text{Cr}} \left[ C_1 - C_2 (X_{\text{Ni}} - C_3)^2 + C_4 (X_{\text{Ni}} - C_3)^4 \right] + 0.08542 X_{\text{Co}}$$

Then using eq(2) to express  $f_{\gamma_1}$  and  $f_{\gamma_2}$ , we obtain:

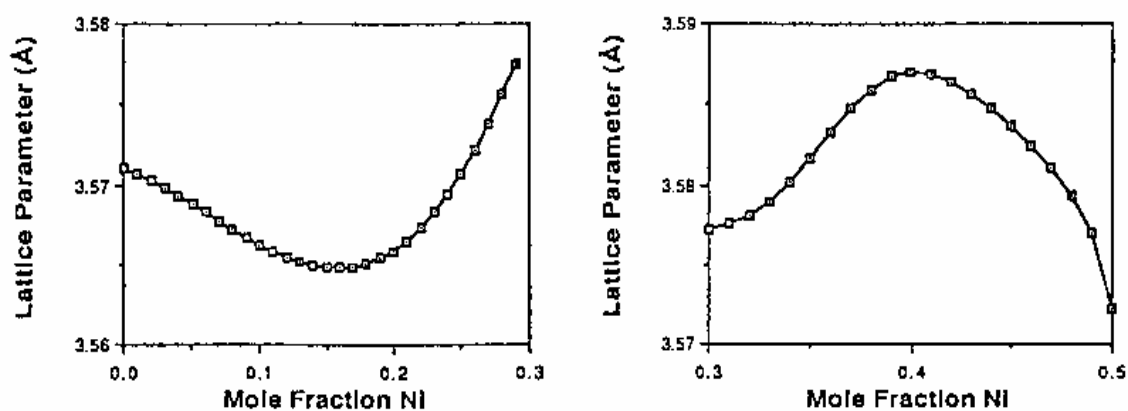


FIG. 3.

Lattice parameter of FCC in the Fe-Ni system for  $X_{Ni} < 0.29$  in (a) and  $X_{Ni} > 0.29$  in (b).

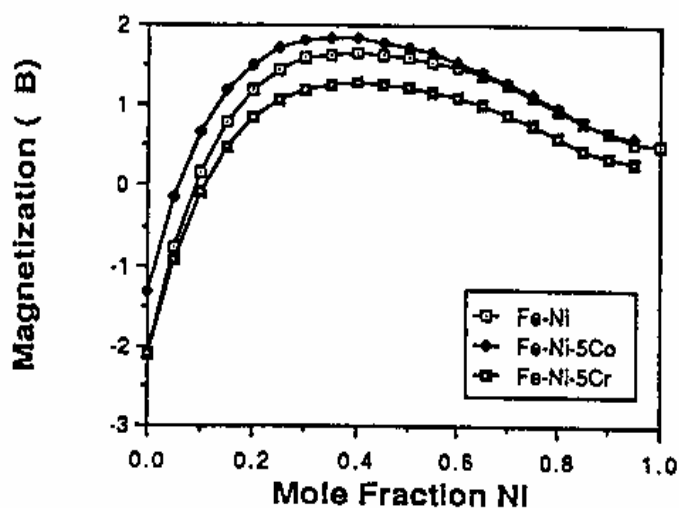


FIG. 4.

Effect of Ni on the magnetic moment (in Bohr magnetons) of the Fe-Ni, Fe-Ni-5Co, and Fe-Ni-5Cr systems evaluated using the THERMOCALC database.

$$\alpha_{\text{FCC}} = 3.514X_{\text{Ni}} + 3.544X_{\text{Co}} + 3.64 \left[ (1 - X_{\text{Ni}} - X_{\text{Co}} - X_{\text{Cr}}) \frac{0.02747(1 - X_{\text{Ni}} - X_{\text{Co}} - X_{\text{Cr}})}{1 + \frac{g_0}{g_1} \exp(\Delta E/RT)} \right] + X_{\text{Cr}} \left[ C_1 - C_2(X_{\text{Ni}} - C_3)^2 + C_4(X_{\text{Ni}} - C_3)^4 \right] + 0.08542 X_{\text{Co}} \quad (9)$$

$\Delta E$  in eq(9) is given by summing the contributions of Ni, Cr, and Co:

$$\Delta E = A + BX_{\text{Ni}} + CX_{\text{Ni}}^2 + DX_{\text{Ni}}^3 + B'X_{\text{Cr}} + C'X_{\text{Cr}}^2 + B''X_{\text{Co}} + C''X_{\text{Co}}^2 + D''X_{\text{Co}}^3$$

where the coefficients have been defined above. Eq(9) is the final equation to be used for the evaluation of the lattice parameter  $\alpha_{\text{FCC}}$  in the Fe-Ni-Cr-Co system.

The value of the lattice parameter for the product phase BCC,  $\alpha_{\text{BCC}}$  is calculated using Vegard's law:

$$\alpha_{\text{BCC}} = \alpha_{\text{Fe}} X_{\text{Fe}} + \alpha_{\text{Ni}} X_{\text{Ni}} + \alpha_{\text{Cr}} X_{\text{Cr}} \quad (10)$$

where  $\alpha_{\text{Cr}} = 2.8846 \text{ \AA}$  for BCC Cr from Barrett and Massalski [13]. Experimental data from Ruhl[9] on the Fe-Ni BCC lattice parameters can be used to further develop eq(10). Ruhl's data for the compositional dependence of the lattice parameter for Ni content higher than 25 atomic percent can be represented by the following equation:

$$\alpha_{\text{BCC}}(\text{Fe-Ni}) = 2.8664 - 0.11(X_{\text{Ni}} - 0.25), \text{ for } X_{\text{Ni}} > 0.25$$

Eq.(10) then becomes:

$$\alpha_{\text{BCC}} = [2.8664 - 0.11(X_{\text{Ni}} - 0.25)](1 - X_{\text{Cr}}) + 2.8846 X_{\text{Cr}} \quad (11)$$

Eq.(11) gives the lattice parameter of Fe-Ni-Cr BCC system for  $X_{\text{Ni}} > 0.25$ . The effect of Co was not taken into account because of the lack of information on the lattice parameter of Fe-Co BCC solid solutions.

Eq.(1),(9), and(11) are then used to evaluate the volume change  $\Delta V/V$  as a function of composition.

The toughening effects discussed in ref.1 were associated with AF1410 steel with strength in the range 45 to 50 Rc. An attempt will be made now to design alloy compositions for transformation toughening in the 50-55 Rc range corresponding to 1700-2100 MPa in tensile strength. The additional mechanical driving force at these higher strengths must be compensated by a corresponding chemical stabilization of the precipitated austenite to ensure similar toughening effects as for AF1410 steel.

The increment in the mechanical driving force  $\Delta(\Delta G^\sigma)$  due to an increment in stress  $\Delta\sigma$ , can be calculated using the Patel-Cohen criterion[14] as:

$$\Delta(\Delta G^\sigma) = (\Delta\sigma) \left( \frac{\partial \Delta G^\sigma}{\partial \sigma} \right)$$

For the crack-tip stress-state,  $\partial \Delta G / \partial \sigma = 1.42 \text{ J/mol.MPa}$ [15]. So for  $\Delta\sigma = 400 \text{ MPa}$ ,  $\Delta(\Delta G^\sigma) = 568 \text{ J/mol}$ . The free energy change for the martensitic transformation evaluated at room temperature for equilibrium austenite precipitated at a tempering temperature of 510°C will be adopted as a measure of stability. This quantity was calculated using the THERMOCALC software with a procedure described in section 2. For AF1410 steel (14Co-10Ni matrix) the free energy change is  $\Delta G_{\text{ch}} = 813 \text{ J/mol}$ . Therefore, in order to compensate for the increment in the mechanical driving force calculated above, the free energy change must increase to 1380 J/mol. The quantity  $\Delta G_{\text{ch}}$  was calculated for several alloy compositions, and the results are listed in Table 3. The compositions of equilibrium austenite are also shown in Table 3. As was mentioned earlier, the selection of alloy compositions is subject to the constraint of a large volume change. Therefore, the transformational volume change was calculated for each of the alloys listed in Table 3, with the aid of eq(1),(9), and (11) of the previous section. Several of the alloys in Table 3 contain Cr. It is important to note that this is the Cr remaining in solution after complete



precipitation of  $M_2C$  carbides at 510°C. The alloy compositions in Table 3 are therefore matrix compositions. The alloy composition in Table 3 that satisfies the stability requirement of 1380J/mol is Fe-14Co-15Ni-2Cr (in wt%) which possesses a  $\Delta G_{ch}$ =1427J/mol and  $\Delta V/V$ =3.3%. Both, the stability and the volume change are much higher than the corresponding values for the reference Fe-14Co-10Ni matrix. It, therefore, represents the alloy matrix composition with the best combination of austenite stability and transformation volume change for enhanced transformation toughening at higher strength levels.

**Table 3** Dependence of austenite stability and transformation volume change on alloy matrix compositions (wt%).

Alloy (Co-Ni-Cr)	Austenite Composition (783K)			$\Delta G_{ch}(300K)$	$\Delta V/V(\%)$
	Ni	Co	Cr		
14-10	0.41	0.032	0	813 J/mol	2.20
16-15	0.43	0.045	0	1300	2.24
14-15-2	0.39	0.044	0.043	1427	3.30
14-13-3	0.37	0.044	0.067	1115	4.1
13-13-3	0.37	0.04	0.066	1045	3.88

#### 4. Conclusions

Dispersed-phase transformation toughening at ultrahigh strength levels can be potentially enhanced by increasing austenite stability and transformation volume change. Computer-aided thermodynamic analysis can be used to predict the effect of composition on austenite stability. The effect of composition on the transformation volume change stems from the compositional dependence of the lattice parameters. A formulation based on the two-gamma states model has been proven useful in predicting the effect of composition on the lattice parameter of austenite.

#### References

1. G.N. Haidemenopoulos, "Dispersed-Phase Transformation Toughening in Ultrahigh-Strength Steels", Doctoral Thesis, MIT, Cambridge, MA, 1988.
2. G.N. Haidemenopoulos, G.B. Olson, and Morris Cohen, "Dispersed-Phase Transformation Toughening in Ultrahigh-Strength Steels", in Proc. 34th Sagamore Army Materials Research Conference on Innovations in Steel Technology, Lake George, NY, August 1987 (in press).
3. C.C. Young, "Sharp-Crack Transformation Toughening in Phospho-Carbide Strengthened Austenitic Steels", Doctoral Thesis, MIT, Cambridge, MA (1987).
4. K.J. Tauer and R.J. Weiss, Bull. Am. Phys. Soc. **6** (1961) 125
5. R.J. Weiss and K.J. Tauer, Phys. Rev. **102** (ii), (1956) 1490.
6. R.J. Weiss and K.J. Tauer, J. Phys. Chem. Solids, **4** (1958) 135.
7. L. Kaufman, E.W. Clougherty, and R.J. Weiss, Acta Metall. **11** (1963) 323.
8. R.J. Weiss, Proc. Phys. Soc., **82** (1963) 281
9. R. Ruhl, " Splat Quenching of Fe-Based Alloys", Doctoral Thesis, MIT, Cambridge, MA, (1967).
10. A.P. Miodownik, Acta Metall., **18** (1970) 541
11. W.B. Pearson, " Handbook of Lattice Spacings", Pergamon Press, London, (1958).
12. B. Sundman, B. Jansson, and J.O. Anderson, CALPHAD, **9** (1985) 153
13. C.S. Barrett and T.B. Massalski, " Structure of Metals", McGraw-Hill Book Company, New York, (1966).
14. J.R. Patel and Morris Cohen, Acta Metall., **1** (1953) 531.
15. G.B. Olson, "Transformation Plasticity and the Stability of Plastic flow", in Deformation Processing and Structure, pp. 391-424; ASM, Metals Park, OH, 1983.

#### Acknowledgments

This research has been supported by NSF-MRL Grant# DMR 84-18718 through the MIT Center for Materials Science and Engineering as part of the Steel Research Group program.